CrystEngComm

HIGHLIGHT

View Article Online
View Journal | View Issue



Cite this: *CrystEngComm*, 2018, **20**, 6109

# Coordination supramolecules with oxazoline-containing ligands

Yong-Qing Huang[a] and Wei-Yin Sun *[b]

Received 5th July 2018,
Accepted 31st August 2018

DOI: 10.1039/c8ce01099d

rsc.li/crystengcomm

Coordination supramolecules (CSs), constructed by assembly of metal ions/clusters (referred to as nodes) and organic bridging ligands (referred to as linkers), are a class of inorganic–organic hybrid materials. The key to construct such functional materials is the careful choice of organic linkers due to their readily tailored nature. The geometry, rigidity and types of organic linkers, especially together with elaborately decorated functional groups, certainly exert influence on the structures of CSs, as well as the structure-driven properties. In this highlight, we will focus on the recent development of CSs with oxazoline-containing ligands, including discrete coordination complexes and coordination polymers. This highlight will be beneficial to researchers attempting the design and synthesis of oxazoline-based CSs.



## 1. Introduction

Coordination supramolecules (CSs) are a class of inorganic–organic hybrid materials that have been proved to be important for both fundamental research and potential applications. In recent years, they have attracted extensive attention due to their diverse and fascinating structures[1] along with interesting properties in gas storage and separation,[2,3] sensing,[4] catalysis,[5] ferroelectronics, non-linear optics and LEDS,[6] and drug delivery.[7] CSs consist of two primary building components: metal ions (primary building unit, PBU) or metal clusters (secondary building unit, SBU), referred to as nodes, and multitopic organic ligands, referred to as linkers, which are combined together through coordination interactions, leading to formation of zero- (0D), one- (1D), two- (2D) and three-dimensional (3D) metal–organic architectures.[8] Theoretically, the combinations between inorganic and organic building units are versatile and limitless, providing a vast stage for researchers to achieve the desired CSs.

Up to now, varied metal ions have been utilized in the construction of CSs, which have different valences and radii, responsible for different affinities for different ligands.[9] Consequently, the metal affinity for ligands plays a vital role aside from the coordination numbers and geometries of metal centers in the crystal engineering and molecular architecture fields. On the other hand, compared to the metal ions and metal clusters, the number of organic linkers is enormous. Furthermore, they can be judiciously tailored by incorporating functional groups into the organic skeleton. Therefore, in the past years, most attention on the CSs has been paid to the synthesis of new bridging organic ligands as well as chemical modifications of the known ligands.[10]

To this day, the reported carboxylate- and/or N-donor-containing ligands occupy a dominant position in the construction of CSs. In contrast to the definite carboxylate group, the N-donor-containing heterocyclic moieties are versatile including pyridine, pyrimidine, imidazole, triazole, tetrazole, imidazoline and so on, which have different N-donor atom numbers, coordination abilities and modes. In addition, the N-donor-containing heterocycles themselves, apart from the ligand skeleton, can be chemically modified enabling us to facilely adjust the steric and electronic behavior of the linkers.[11] Among the N-donor-containing heterocyclic ligands, to date, the use of oxazoline-based ligands as linkers is relatively limited in crystal engineering and molecular

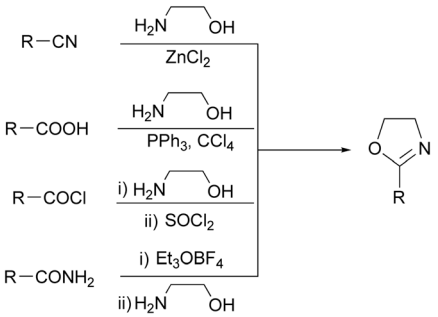


**Scheme 1** Typical synthetic methods for 2-oxazolines. Adapted from ref. 13*b*.

[a] *State Key Laboratory of Mining Disaster Prevention and Control Co-founded by Shandong Province and the Ministry of Science and Technology, College of Chemical and Environmental Engineering, Shandong University of Science and Technology, Qingdao 266590, China*
[b] *Coordination Chemistry Institute, State Key Laboratory of Coordination Chemistry, School of Chemistry and Chemical Engineering, Nanjing National Laboratory of Microstructures, Collaborative Innovation Center of Advanced Microstructures, Nanjing University, Nanjing 210023, China. E-mail: sunwy@nju.edu.cn*

architecture fields, although they have been widely employed in asymmetric catalytic processes mainly as the chiral auxiliaries.[12] From another perspective, this provides a huge ligand candidate pool for researchers, facilitating the design and synthesis of oxazoline-containing bridging ligands. On the other hand, as shown in catalysis, oxazoline-containing ligands have their own advantages compared with other N-donor-containing heterocyclic ligands: the synthesis is facile because they can be directly synthesized from carboxylate derivatives or nitriles and aminoalcohols that are readily available by reduction of α-amino acid (Scheme 1). Moreover, there are abundant chiral α-amino acids in nature, which can be conveniently employed to prepare chiral oxazoline-containing ligands with the stereocenter close to the N-donor atom.[13] Obviously, these advantages are also valid for the construction of CSs, particularly chiral CSs.

Oxazolines, commonly known as 2-oxazolines, can be regarded as hydrogenated oxazoles, which possess one soft σ-donor N atom compared with other azoles and azolines and incline to coordinate with soft Lewis $d^{10}$ metal cations such as Ag(I), Cu(I) and Hg(II) rather than hard ones like lanthanide [Ln(III)]. However, by taking advantage of the chelating effect, oxazoline groups which are difficult to bind to hard metal ions can be successfully solved by using chelate oxazoline-containing ligands.[14] It means that there are remarkable differences between the coordination behaviors of oxazoline- and imidazole-containing ligands, even though both oxazoline and imidazole are N-donor containing five-membered rings.

In this highlight, we will focus our attention on the latest developments in the structures and properties of oxazoline-based CSs with definite structures, including discrete coordination complexes and 1D and 2D coordination polymers (CPs). We hope that this highlight will be beneficial to chemists for the design and construction of targeted oxazoline-based CSs with desired properties.

## 2. Discrete coordination complexes based on oxazoline-containing ligands

Varied synthetic strategies including the symmetry interaction model, molecular library model, molecular panelling model and molecular clip approach have been utilized to construct molecular coordination architectures with specific geometries.[15]

### 2.1. Homoleptic discrete oxazoline-based coordination complexes with transition metal ions

A molecular clip approach based on ligand symmetry directed interactions has been used to construct supramolecular cages, rectangles, *etc.* For example, $C_3$-symmetric disk-shaped tri-monodentate ligands combined with 2-connected metal nodes produce $M_3L_2$ type cages.[15f,16] In 2002, Hong *et al.* reported the first enantiomerically pure propeller-shaped $M_3L_2$ supramolecular cage *M*-$[Ag_3(L1^S)_2]^{3+}$ (**1**) with $C_3$-symmetric chiral ligand (*S*)-1,3,5-tris(4-methyl-oxazolin-2-yl)-benzene ($L1^S$) (Scheme 2).[17] As reported, the helical supramolecular cage **1** was readily achieved by mixing chiral tri-monodentate tris(oxazoline) ligand $L1^S$ and labile Ag(I) as a 2-connected node in a 2 : 3 ratio. It is worth noting that the chirality of propeller-shaped $[Ag_3(L1)_2]^{3+}$ originates from the chiral ligand since $[Ag_3(L1^S)_2]^{3+}$ presents only the *M*-form and $[Ag_3(L1^R)_2]^{3+}$ (**2**) shows only the *P*-form. In addition, in a racemic mixture of chiral L1 ligands and $AgNO_3$, exclusive ligand self-recognition was observed, which was ensured by $^1$H NMR spectroscopy and single crystal X-ray diffraction analysis. More importantly, the chirality of $[Ag_3(L1)_2]^{3+}$ induced by chiral ligands was further confirmed by later work.[18] When achiral analogous ligand 1,3,5-tris(2-oxazolin-2-yl)-benzene (L2) was utilized to react with Ag(I)/Cu(I) perchlorate, two similar *meso* propeller-shaped $[M_3(L2)_2]^{3+}$ cages [**3**, M = Ag(I); **4**, M = Cu(I)] were isolated with *P*- and *M*-configurational cages in a 1 : 1 ratio and *PMPM* stacking mode. The results show that the formation of propeller-shaped cages relies on the rigid ligands as well as the *ortho*-positioned N-donor atoms, which can be further ascertained by the following examples **6**–**11**. When a similar $C_3$-symmetric disk-shaped tri-monodentate imidazole ligand 1,3,5-tris(1-imidazolyl)benzene (tib) with *meta*-positioned N-donor atoms was used to react with Ag(I) salts, no propeller-shaped $M_3L_2$ cages were obtained,[19] whereas the reaction of flexible $C_3$-symmetric tripodal ligand 1,3,5-tris(imidazol-1-ylmethyl)-2,4,6-trimethylbenzene (timtmb) with silver(I) salts can generate $M_3L_2$ triangular prisms rather than propeller-shaped $M_3L_2$ cages.[20] On the other hand, it is known that the assembly of CSs can be influenced by varied factors including counter anions. An $M_2L_2$ macrocycle $[Cu_2(L2)_2]^{2+}$ (**5**) was obtained by addition of CuBr in the preparation reaction, in which one oxazoline group of L2 did not participate in the coordination with Cu(I) ions.[18b] Namely, L2 ligands act as bis-monodentate bridging ligands to link two 2-connected Cu(I) ions to generate a 16-membered metallocycle.

In addition to the aforementioned $C_3$-symmetric tri-monodentate oxazoline-containing ligands, a $C_3$-symmetric hexa(oxazoline) ligand (L3) with alternately arranged oxazolinyl and oxazolinylphenyl groups outlined in two circles has been deliberately designed and synthesized. By using the L3 ligand to react with Ag(I) and Hg(II) salts, Shionoya *et al.* reported a hetero-metal $[Ag_3Hg_3(L3)_2]^{9+}$ (**6**) supramolecular

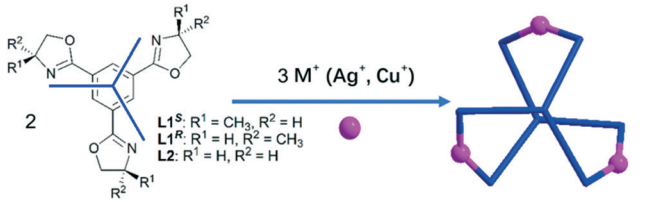


**Scheme 2** Schematic representation for the synthesis of propeller-shaped $M_3L_2$ cages **1**–**4** from ligands L1 and L2. Adapted from ref. 17 and 18.

 

cage with a hierarchical array of Ag(I) and Hg(II) ions (Fig. 1).[21] Further studies revealed that the specific hierarchical arrangement is attributed to the larger electrostatic repulsion between Hg(II) ions than that between Ag(I) ions, together with the stronger binding affinity between Hg(II) and oxazoline groups than that between Ag(I) and oxazoline groups. Meanwhile, the formation of **6** was investigated in detail as illustrated in Fig. 1. Furthermore, for comparison, three homometal $M_3L_2$ cages $[Ag_3(L4)_2]^{3+}$ (**7**) and $[M_3(L5)_2]^{3+}$ [M = Ag(I) (**8**), Cu(I) (**9**)] were prepared by using disk-shaped tri-monodentate oxazoline-based ligands L4 and L5 as depicted in Scheme 3.

To further study the arrays of two distinct $d^{10}$ metal ions on a circle and understand the assembly mechanism, two rigid $C_6$-symmetric ligands hexa(4-(4,4-dimethyl-oxazolin-2-yl)phenyl)benzene (L6) and hexa(4-(oxazolin-2-yl)phenyl)-benzene (L7) were designed and two $[M_3Hg_3(L6)_2]^{9+}$ [M = Ag(I) (**10**), Cu(I) (**11**)] supramolecular cages, accompanied with three M(I) (M = Ag, Cu) and three M(II) (M = Hg) alternately arrayed on a concentric circle, were achieved (Fig. 2).[22]

In addition to the above mentioned $C_3$ and $C_6$ ligands with high symmetry, low symmetric oxazoline-based ligands can also be employed to build discrete supramolecular complexes. For instance, in 2010, we designed a flexible bridging ligand *N,N'*-bis(4-(2-oxazolinyl)benzyl)ethane-1,2-diamine (L8) (Scheme 4) and used it to react with Ag(I) and Cu(II) salts to generate an $M_2L_2$ molecular rectangle $[Ag_2(L8)_2](NO_3)_2 \cdot 4CH_3NO_2$ (**12**) and an $M_4L_2$ molecular cage $[Cu_4(L8)_2(OCH_3)_2(OH)_2(NO_3)_2](NO_3)_2 \cdot 0.32H_2O$ (**13**).[23] In the case of **12**, two L8 ligands, acting as bis-monodentate ligands, combine with two linear Ag(I) to form a metallocyclic rectangle with side lengths of 16.36 × 6.30 Å$^2$, while in the case of **13**, two L8 ligands, serving as U-shaped tetradentate ligands, connect with two dinuclear Cu(II) cores to give a novel $M_4L_2$ cage. It is noteworthy that in contrast to the NO coordination of the ethane-1,2-diamine unit in L8 with Ag(I) in **12**, the ethane-1,2-diamine unit in **13** binds to a Cu(II) ion as a chelating ligand.

Aside from the flexible L8 ligand, in 2012, a rigid $C_2$-symmetric ligand 1,3-bis(oxazolin-2-yl)benzene (L9) (Scheme 5) was used to react with six different silver(I) salts, leading to the formation of six CSs $[Ag_2(L9)_2](NO_3)_2$ (**14**), $[Ag_2(L9)_2](ClO_4)_2$ (**15**), $[Ag_2(L9)_2(CH_3SO_3)_2](CH_3OH)_2$ (**16**), $[Ag_2(L9)_2(CF_3SO_3)_2]$ (**17**), $[Ag_2(L9)_2(CH_3CN)_2](PF_6)_2$ (**18**), and $[Ag_3(L9)_4](SbF_6)_3$ (**19**).[24] Complexes **14–18** have similar 16-membered $M_2L_2$ metallocyclic structures to **5**, while **19** features a novel $M_3L_4$ structure with Ag(I)-shared two interconnected 16-membered rings as exhibited in Scheme 5, however, they show different 3D packing structures derived from different sizes, shapes, coordinations and hydrogen bonding abilities of the counter anions. In the cases of isostructural anions $CF_3SO_3^-$ and $CH_3SO_3^-$, both act as terminal ligands due to their stronger coordination ability than the other four counter anions $ClO_4^-$, $NO_3^-$, $PF_6^-$ and $SbF_6^-$. Furthermore, the formation of the $M_3L_4$ structure of **19** may be ascribed to the large size and volume of $SbF_6^-$.

Replacement of the benzene ring in L9 with the pyridine ring gives another $C_2$-symmetric ligand 2,6-bis(oxazolin-2-yl)-pyridine (pybox). In catalytic studies, pybox derivatives have been widely used as tri-dentate chelating ligands to generate varied catalysts. In contrast, chiral pybox derivatives have been successfully used to construct optically pure CSs as bis-monodentate ligands without coordination of the pyridine N-donor atom.[25]

In fact, as early as 1997, Williams and co-workers employed two chiral pybox derivative ligands L10 and L11 to react with $AgBF_4$ in a 1 : 1 ligand-to-metal ratio, affording chiral double and triple helicates $[Ag_2(L10)_2](BF_4)_2$ (**20**) and $[Ag_3(L11)_3](BF_4)_3$ (**21**), respectively (Scheme 6).[25a] In the case

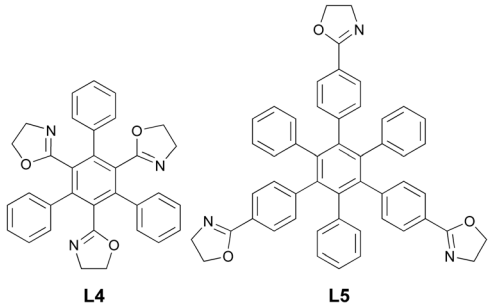


**Scheme 3** Schematic drawing for ligands L4 and L5. Adapted from ref. 21.

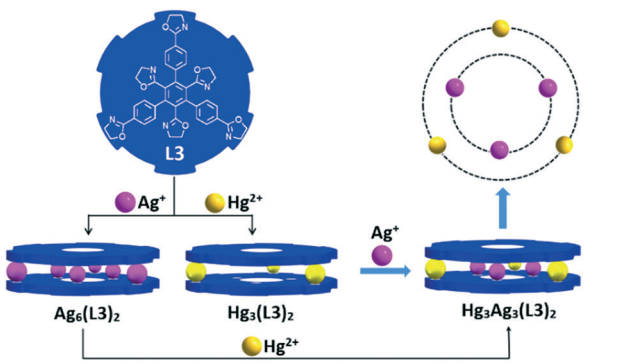


**Fig. 1** Schematic representation of the hierarchical arrangement of Ag(I) and Hg(II) between two hexa-monodentate L3 ligands in **6**. Adapted from ref. 21.

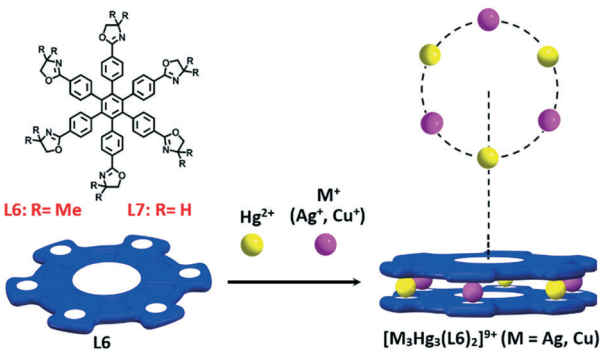


**Fig. 2** Schematic representation of the alternate arrangement of M(I) (M = Ag, Cu) and Hg(II) ions to form hetero-metal hexanuclear $[M_3Hg_3(L6)_2]^{9+}$ cages **10** and **11**. Adapted from ref. 22.

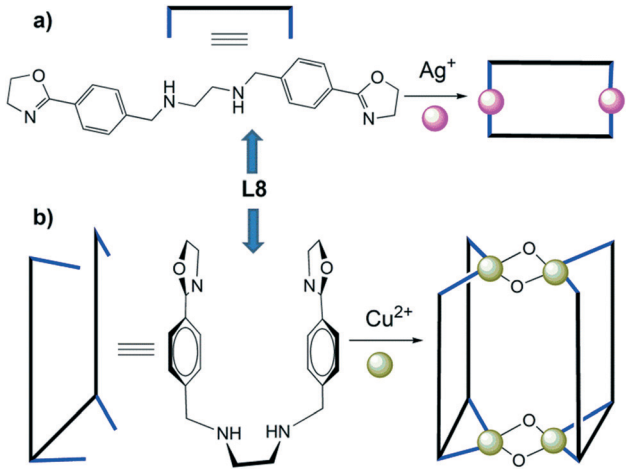


**Scheme 4** Schematic drawing for the synthesis of rectangle **12** (a) and cage **13** (b) with the L8 ligand. Adapted from ref. 23.

of **20**, two Ag(I) ions, located on the pseudo-twofold axes, are wrapped by two twisted L10 ligands (Fig. 3a). In contrast, **21** is made up of an equilateral triangle of Ag(I) ions, which are linked together by three bridging L11 ligands tilted in one direction (Fig. 3b). Recently, Gamasa *et al.* used a pybox derivative ligand 2,6-bis[(3aS,8aR)-8,8adihydro-3aH-indeno[1,2-d]oxazol-2-yl]-pyridine (L12) and three different Ag(I) salts in a 3 : 2 ratio to construct three optically pure $[Ag_2(L12)_3][X]_2$ triple-stranded helicates [X = $CF_3SO_3$ (**22**), $SbF_6$ (**23**), and $PF_6$ (**24**)] rather than mononuclear or dinuclear complexes in different L : M ratios (Scheme 6 and Fig. 3c). Among them, L12 ligands take a twisted bis-monodentate bridging mode to connect two three-coordinated Ag(I) ions.

### 2.2. Homoleptic discrete oxazoline-based coordination complexes with $Ln^{3+}$ ions

In contrast to the well-used d-block transition metal ions, $Ln^{3+}$ ions are relatively less employed in the construction of discrete CSs with specific geometries. The main reasons are attributed to the inherent varied coordination numbers, weak stereochemical preference and kinetic lability of $Ln^{3+}$. Additionally, the hard acid nature of $Ln^{3+}$ ions makes them difficult to bind with soft bases like oxazoline N-donor atoms.

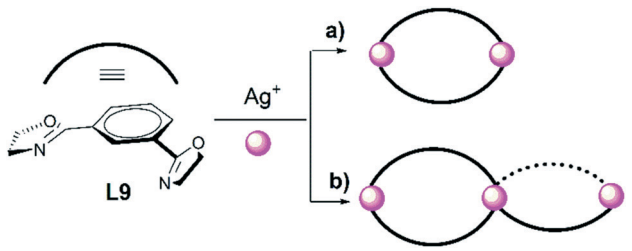


**Scheme 5** Schematic drawing for the 16-membered metallocycles **14**–**18** (a) and the $M_3L_4$ structure with two inter-connected rings **19** (b). Adapted from ref. 24.

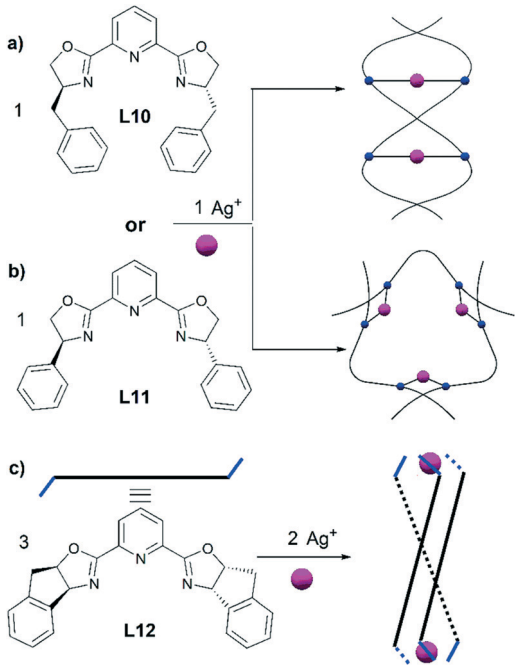


**Scheme 6** Schematic drawing for the synthesis of $M_2L_2$ (**20**) (a), $M_3L_3$ (**21**) (b) and $M_2L_3$ (**22**–**24**) (c) helicates. Adapted from ref. 25.

To achieve discrete CSs and prevent the formation of CPs, symmetric multi-topic ligands with oxazoline-containing chelating units have been used to react with $Ln^{3+}$ salts.[26] This synthetic strategy is also called the symmetry interaction model. For example, by using analogue bis-tridentate oxazoline-containing ligands L13 and L14 with 1,5-diaminonaphathalene and benzidine as spacers, respectively, (Scheme 7) and $Eu(OTf)_3$, two triple-stranded helicates $[Eu_2(L13)_3]^{6+}$ (**25**) and $[Eu_2(L14)_3]^{6+}$ (**26**) were afforded in low concentration, whereas in high concentration, a new tetrahedral cage $[Eu_4(L13)_6]^{6+}$ (**27**) appeared (Scheme 7 and Fig. 4a).[26] In other words, triple-stranded helicate **25** and tetrahedral cage **27** can be converted to each other by changing the concentration. In addition to the $M_4L_6$ type tetrahedron **27**, in the same year, two isostructural $M_4L_4$ tetrahedral cages $[Eu_4(L15)_4]^{6+}$ (**28**) and $[Eu_4(L16)_4]^{6+}$ (**29**) were obtained by assembly reactions of tris-tridentate oxazoline-based ligands L15 and L16 with $Eu(OTf)_3$, respectively (Scheme 8).[26b] According to the $^1H$ NMR and ESI-TOF-MS data, both **28** and **29** exist in solution. Moreover, the crystal structure of **28**

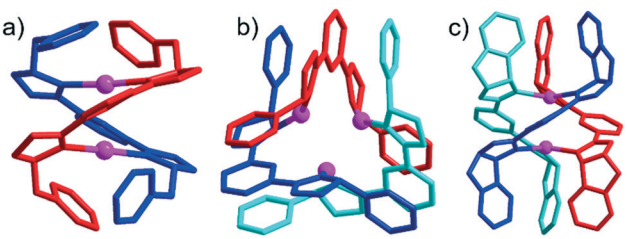


**Fig. 3** Crystal structures of helicates **20** (a), **21** (b) and **22** (c). Adapted from ref. 25.

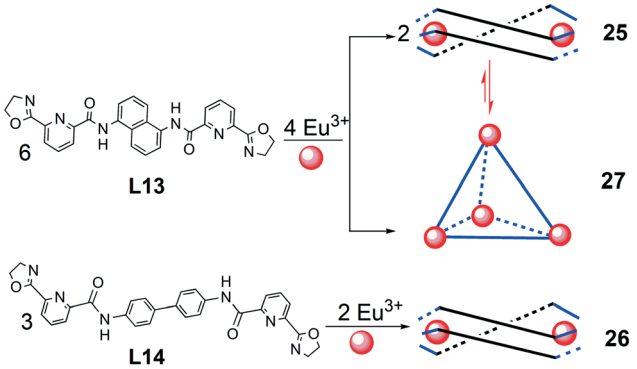


**Scheme 7** Schematic representation for the synthesis of $M_2L_3$ helicates **25**, **26** and $M_4L_6$ tetrahedron **27** from L13 and L14. Adapted from ref. 26*a*.

further ensured the formation of the $M_4L_4$ tetrahedral cage in the solid state (Fig. 4b).

Compared with the well-used symmetry interaction model using multi-topic chelating ligands, Mazzanti and his co-workers employed a metal-directed method using asymmetric multidentate ligands to generate polynuclear Ln-based CSs.[27] For instance, they designed and synthesized two asymmetric chiral tetradentate oxazoline-containing ligands (*R*/*S*)-6′-(4-phenyloxazolin-2-yl)-2,2′-bipyridine-6-carboxylate ($L17^{R/S}$) to build Eu-oxazoline-containing CSs. Following this synthetic strategy, two enantiopure trinuclear triangles: (ΔΔΔ)-$[Eu(L17^S)_2]_3^{3+}$ (**30**) and (ΛΛΛ)-$[Eu(L17^R)_2]_3^{3+}$ (**31**) and two heptanuclear wheels [Eu ⊂ (Δ-$Eu(L17^S)_2$Λ-$Eu(L17^S)_2)_3$](OTf)$_9$ (**32**) and [Eu ⊂ (Λ-$Eu(L17^R)_2$Δ-$Eu(L17^R)_2)_3$](OTf)$_9$ (**33**) have been successfully obtained.[27c,d] Notably, during the assembly process, steric constraints caused by the phenyl groups on the oxazoline rings result in the formation of diastereoselective homochiral triangles **30** and **31**. It is interesting that the chiral trinuclear triangles and heptameric wheels can interconvert, which are controlled by the $Eu^{3+}$ concentration (Scheme 9).

### 2.3. Heteroleptic discrete oxazoline-based coordination complexes

In addition to the above described coordination complexes, each with only one kind of oxazoline-containing ligand, the combination of mixed organic ligands, including at least one oxazoline-containing ligand, with transition metal ions may generate more complicated coordination-driven supramolecules and molecular devices. Hong *et al.* successfully constructed a hamburger-shaped coordination complex *M*-$[Ag_6(L18^R)_2(tbib)]^{3+}$ (**34**) with unidirectional helicity (Scheme 10). **34** consists of chiral $C_3$-symmetric tri-monodentate tris(oxazoline) ($L18^R$) and achiral tris-(benzimidazoline)benzene (tbib) with a ratio of 2 : 1, connected through six 2-coordinated Ag(I) ions.[28] The left-handed helicity of **34** relies on the chirality of $L18^R$, which facilitates the formation of CH–π hydrogen bonds and avoids steric repulsion. Additionally, it is notable that deprotonated tbib acting as a bis(tris-monodentate) ligand plays a key role in the formation of hamburger-shaped supramolecule **34**.

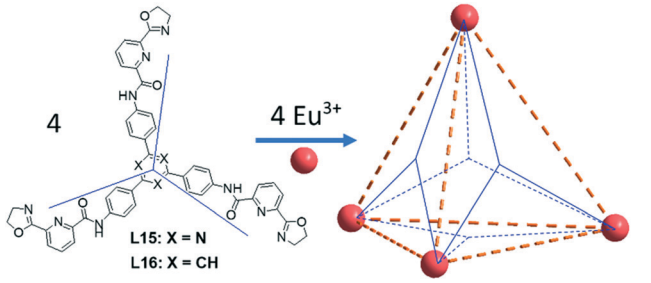


**Scheme 8** Schematic drawing for the synthesis of $M_4L_4$ tetrahedral cages **28** and **29** from ligands L15 and L16. Adapted from ref. 26*b*.

### 2.4. Oxazoline-based coordination supramolecular devices

Through ingenious design, heteroleptic CSs with multi-decker structures can serve as molecular devices based on molecular motion in solution as reported by Shionoya and his co-workers.[29] In 2004, they reported a molecular ball bearing $[Ag_3(L19^S)(htb)]^{3+}$ (**35**), obtained by association of a hexa-monodentate thiazolyl ligand (htb) and a chiral tris-monodentate oxazolyl ligand ($L19^S$) in a 1 : 1 ratio with three Ag(I) ions. In $CD_3OD$ solution, two disk-shaped ligands htb and $L19^S$ in **35** can reversely rotate with equal probability,

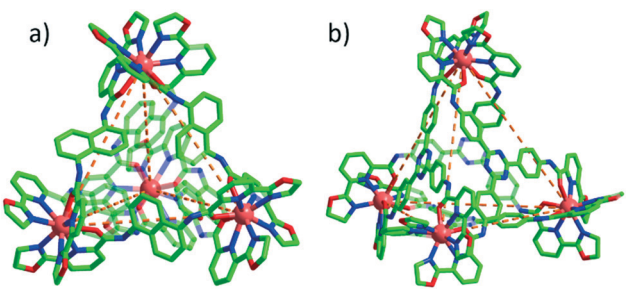


**Fig. 4** Crystal structures of tetrahedral cages **27** (a) and **28** (b). Adapted from ref. 26.

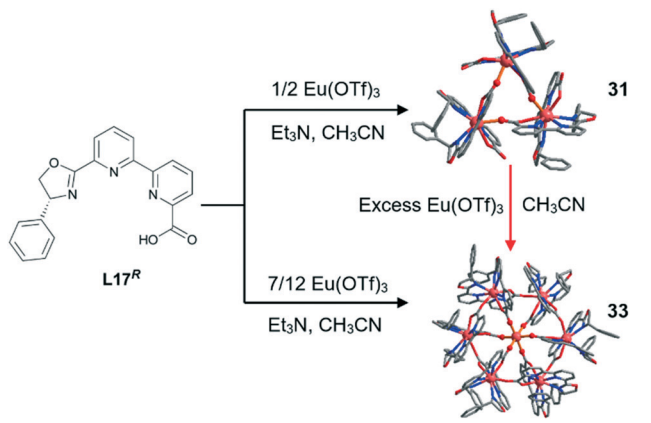


**Scheme 9** Synthesis of enantiopure Eu(III)-based trinuclear triangle **31** and heptameric wheel **33**. Adapted from ref. 27*c* and *d*.

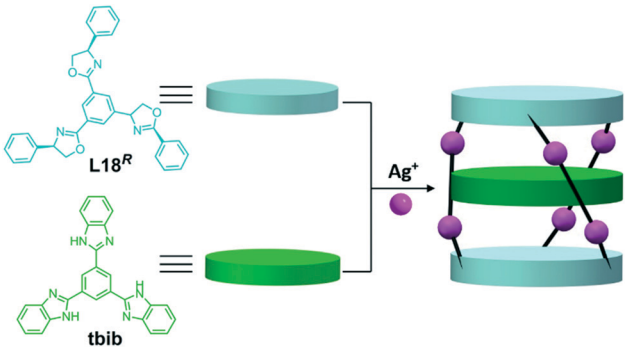


Scheme 10 Schematic representation for synthesis of hamburger-shaped coordination supramolecule **34**. Adapted from ref. 28.

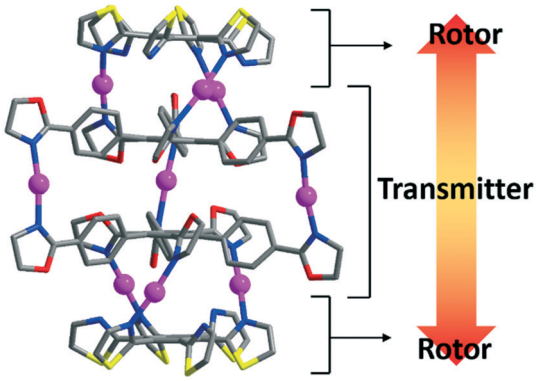


Fig. 5 Crystal structure of **36** showing the molecular rotor–transmitter–rotor device. Adapted from ref. 29*b*.



which was realized by the successive ligand exchange and concurrent flip motions (Scheme 11).[29a] In fact, the coexistence of *P*- and *M*-configurational helical cages of $[Ag_3(L2)_2]^{3+}$ (**3**) or $[Cu_3(L2)_2]^{3+}$ (**4**) in one crystal is just the manifestation of such flip movements.[18] Interestingly, on the basis of such a molecular ball bearing, to replace the tris-monodentate oxazolyl ligand ($L19^S$) with the $C_3$-symmetric hexa(oxazoline) ligand (L3), two quadruple-decker complexes $[Ag_6M_3(L3)_2(htb)_2]^{(6+3n)+}$ [$M^{n+}$ = $Ag^+$ (**36**), $Hg^{2+}$ (**37**)] as displayed in Fig. 5 were achieved, which can be considered as the assembly of two molecular ball bearings mediated by three $Ag^+$ or $Hg^{2+}$ ions.[29b] In other words, the in-between part $[Ag_6M_3(L3)_2]^{(6+3n)+}$ (M = Ag or Hg) can be regarded as the transmitter in solution, which correlates the motions of two rotor htb molecules through helix inversion between helical *P* and *M* isomers. In brief, both molecular ball bearing and rotor-transmitter-rotor rely on the inter-transformation between *P* and *M* forms of propeller-shaped $M_3L_2$ cages.

## 3. Coordination polymers with oxazoline-containing ligands

Oxazoline-containing ligands serve mainly as neutral ligands in the assembly of CPs. Thus, to balance the positive charges of metal ions, counter anions must participate in the formation of CPs as either guest anions or terminal/bridging ligands; accordingly the counter anions may have subtle but important influence on the final structures of CPs. In addition to the counter anions, 4-substituted groups of oxazoline located near the donor-N atom can also affect the final structures of CPs due to the steric hindrance. In addition, most of the reported oxazoline-containing ligands used in the assembly of CPs are homogeneous ditopic and $C_3$-symmetric tritopic linkers. Only limited heterogeneous oxazoline-based ligands are employed in the construction of CPs.

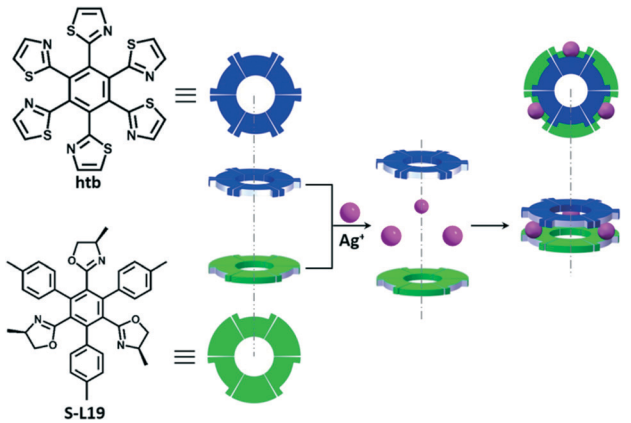


Scheme 11 Schematic drawing of molecular ball bearing **35**. Adapted from ref. 29*a*.

### 3.1. Homoleptic coordination polymers with ditopic oxazoline-based ligands

Aside from the helicates illustrated in Scheme 6 and Fig. 3, the assembly of twisted $C_2$-symmetric bis(oxazoline) ligands with 2-connected nodes can afford 1D helical or 1D zigzag chains. And on this basis, by using chiral bis(oxazoline) ligands, the corresponding stereospecific 1D chains can be realized.

As depicted in Scheme 12, three chiral bis(oxazoline) ligands L20–L22 are all derivatives of 2,2-bis(oxazolin-2-yl)-propane, which have been used as bis-monodentate linkers to react with 2-connected $d^{10}$ $M^+$ ($M^+$ = $Cu^+$ and $Ag^+$) ions, affording three chiral 1D chains $[Cu(L20^{SS})]OTf$ (**38**), $[Ag(L21^{SS})]OTf$ (**39**) and $[Ag(L22^{SS})]OTf$ (**40**).[30] It is interesting that, although $Cu^+$ and $Ag^+$ ions all take nearly linear coordination geometries, **38–40** exhibit totally different structures from each other. **38** and **39** feature 1D helical chain structures with threefold and twofold symmetry, respectively, whereas **40** is a 1D zigzag chain. The structural differences among them may result from the different steric hindrances of 4-substituted groups of oxazoline. In addition, the spacer between the two oxazoline groups in L20–L22 is isopropylidene, which is smaller than the pyridyl spacer in ligands L10–L12, resulting in a larger steric hindrance of L20–L22 than that of L10–L12. Thus, the two oxazoline moieties in ligands L20–L22 take the *exo*-configuration in the 1D chains of **38–40** owing to the large steric hindrance

 

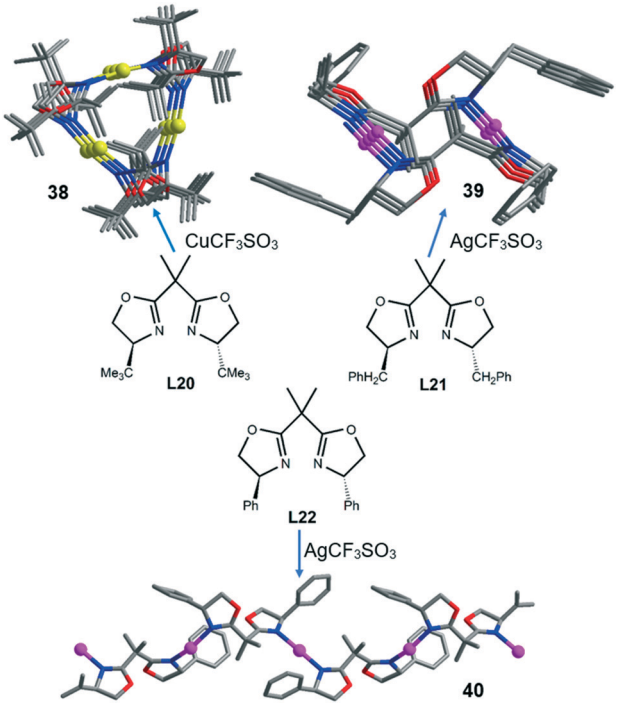


**Scheme 12** Schematic representation for the synthesis of 1D helical chains **38** and **39** and 1D zigzag chain **40** from ligands L20, L21 and L22. Adapted from ref. 30.

(Scheme 12), rather than the *endo*-one which appeared for L10–L12 in **20–24** (Fig. 3), together with L9, L23 and L24 in the following complexes **41–44**.

Replacing the $-C(CH_3)_2-$ spacer between the two oxazoline groups in ligands L20–L22 with a benzene or pyridine group, larger $C_2$-symmetric bis(oxazoline) ligands for example the above-mentioned L9, 1,3-bis[4-(S)-isopropyloxazolin-2-yl]-benzene (L23) and 2,6-di(oxazolin-2-yl)-pyridine (L24) can be obtained (Scheme 13). For these bis(oxazoline) ligands, once the two oxazolinyl groups adopt a *cis*,*trans*-conformation, they will exhibit a twisted nature, which allows them to easily form a helical structure with a 2-connected linear Ag(I) node. In 2011, we used L9 and $AgBF_4$ to construct a new complex $[Ag_4(L9)_4(BF_4)_4]$ (**41**) with 1D left- and right-handed helical chains (Fig. 6).[31] It is noteworthy that the synthetic conditions of **41** are the same as those for **14–19**. Apparently, they show significantly distinct structures: helical chain **41** *vs.* 16-membered cyclic CSs **14–19**, resulting from the different counter anions. Interestingly, **41** crystallizes in the acentric space group *Cc*, which may show nonlinear optical (NLO)

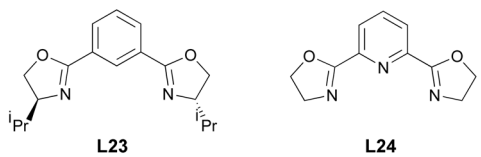


**Scheme 13** Schematic drawing for ligands L23 and L24. Adapted from ref. 32 and 33.

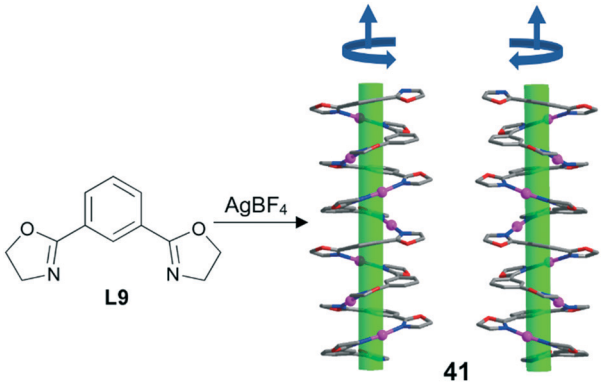


**Fig. 6** Left- and right-handed helical chains in **41** with ligand L9. Adapted from ref. 31.

and ferroelectric properties. The experimental results prove that **41** has modest SHG activity and ferroelectric behavior. In 2015, Gamasa and co-workers employed an analogous chiral bis(oxazoline) ligand L23 to react with $AgPF_6$, yielding an irregular chiral screw chain $[Ag_4(L23)_4](PF_6)_4$ (**42**).[32] Intriguingly, the 1D chains in **41** take a parallel packing mode, while the 1D chains in **42** adopt a plywood-like stacking fashion. In addition, two 1D helical chains, namely $[Ag_5(L24)_5](BF_4)_5$ (**43**) and $[Ag(L24)](SbF_6)$ (**44**), similar to **41**, have been yielded by reaction of achiral pybox ligand L24 and the corresponding silver salts.[33] Notably, the pybox ligand L24 adopts a bis-monodentate bridging mode like that of L9 rather than a tridentate chelating mode. Interestingly, **44** crystallizes in the chiral space group $C222_1$, which means that conglomerate crystallization occurred, in line with its circular dichroism (CD) signal. The second-order NLO measurements suggest that **44** has a stronger SHG intensity than **41**. Furthermore, the ferroelectric measurement of **44** exhibits an electric hysteresis loop.

In addition to angular ditopic oxazoline-based ligands, rod-like ditopic ones are another type of excellent bridging ligand. A rod-like ligand 1,4-bis(oxazolin-yl)-benzene (L25) and its corresponding four CPs $[Ag(L25)(NO_3)]$ (**45**), $[Ag_2(L25)_3](BF_4)_2$ (**46**), $[Ag_2(L25)_3](PF_6)_2$ (**47**) and $[Ag_2(L25)(CF_3CO_2)_2]$ (**48**) were prepared and characterized (Fig. 7).[34] **45** has a 1D zigzag chain structure, in which nitrate anions serve as terminal ligands, while **46** and **47** feature an identical (6,3) topological 2D layer structure, in which counter anions $BF_4^-$ and $PF_6^-$ do not participate in the coordination. In contrast to **46** and **47**, **48** also possesses a 2D organic–inorganic hybrid layer structure, consisting of 1D inorganic $[Ag_2(CF_3CO_2)_2]$ chains and bis-monodentate bridging L25 ligands. Since the synthetic conditions are identical for **45–48**, evidently, the structure differences are ascribed to the different coordination abilities of counter anions. As a continuation of this work, in 2014, a longer rod-like ligand 1,4-bis(oxazolin-yl)-biphenyl (L26) (Fig. 8) was designed and the effect of reaction media on the structures was investigated, thereby yielding three Ag(I) CPs: $[Ag_2(L26)_2(CF_3CO_2)_2]$ (**49**), $[Ag(L26)_{0.5}(CF_3CO_2)]$ (**50**) and $[Ag(L26)_2](CF_3CO_2)(H_2O)_2]$ (**51**).[35] **49** displays a novel great

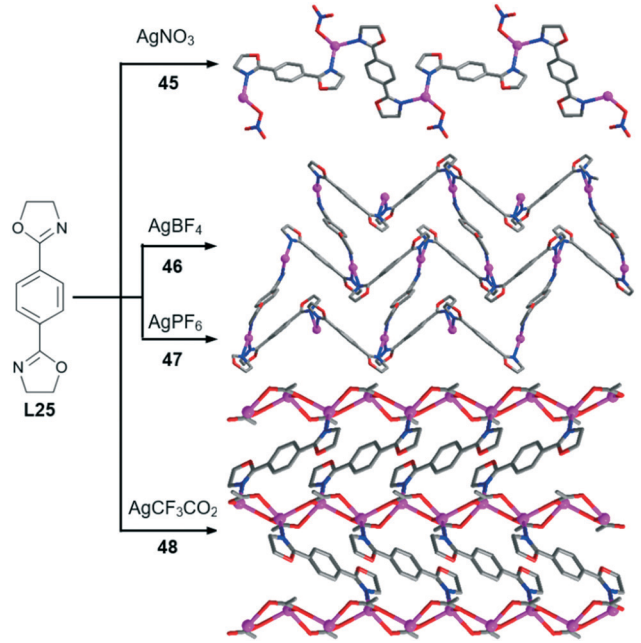


Fig. 7 Crystal structures of CPs **45**–**48** with ligand L25. Adapted from ref. 34.

wall-like 1D chain structure rather than an $M_2L_2$ metallocycle, in which L26 takes a *cis*,*cis*-conformation. **50** has a 2D layer structure similar to that of **48**, in which L26 shows a *cis*, *trans*-conformation. Considering that **49** and **50** have the same chemical components and distinct structures, apparently, they are conformational supramolecular isomers. **51** possesses a (4,4) topological 2D network, in which $CF_3COO^-$ anions act as guest counter ions (Fig. 8).

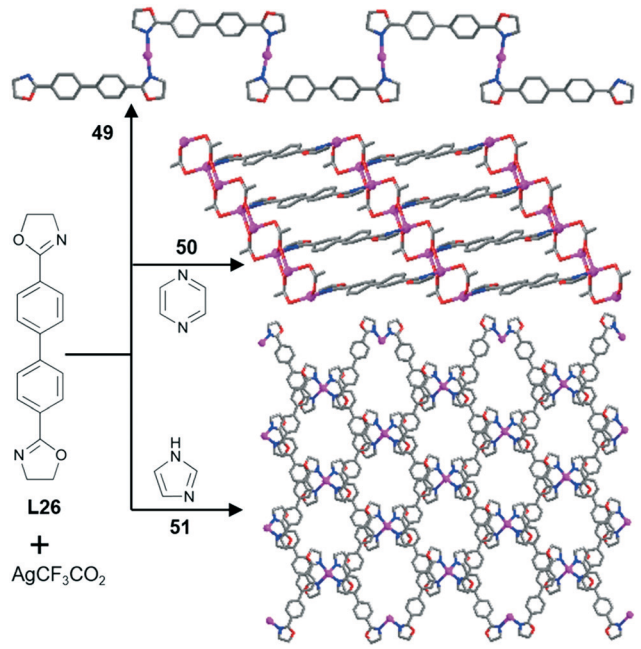


Fig. 8 Crystal structures of CPs **49**–**51** with ligand L26. Adapted from ref. 35.

### 3.2. Homoleptic coordination polymers with tritopic oxazoline-based ligands

As described in section 2.1, $C_3$-symmetric oxazoline-based ligands with a *cis*,*cis*,*cis*-conformation have been widely utilized in the construction of discrete CSs. Yet, when such oxazoline-containing ligands take a *cis*,*trans*,*trans*-conformation, they can act as bridging ligands to construct CPs. Starting from the L2 ligand, seven Ag(I) CPs, $[Ag_2(L2)_2(CF_3SO_3)_2]$ (**52**), $[Ag_2(L2)_2(CH_3SO_3)_2]$ (**53**), $[Ag_2(L2)_2](BF_4)_2$ (**54**), $[Ag_2(L2)_2](ClO_4)_2$ (**55**), $[Ag_3(L2)_2(NO_3)_2]NO_3{\cdot}5H_2O$ (**56**), $[Ag_2(L2)(NO_3)_2]{\cdot}CH_3OH$ (**57**) and $[Ag_4(L2)_2(CH_3CN)_2(CF_3CO_2)_4]$ (**58**), were successfully isolated (Fig. 9).[18a,36] Results of crystal structural analyses revealed that they all have 1D chain structures, which can be viewed as the connection of basic 16-membered metallocycles through different bridging modes. For **52** and **53**, they have the same structures, in which each L2 ligand takes a bis-monodentate bridging mode with the *cis*-arm being non-coordinated. Such two L2 ligands with a *gauche* arrangement linked by two Ag(I) ions first form an $M_2L_2$ ring, which is further joined together by trifluoromethylsulfate or methylsulfate anions in a double bridging fashion to generate two isostructural 1D chains. It is noticeable that two isostructural anions $CF_3SO_3^-$ and $CH_3SO_3^-$ take the mono-atom bridging mode to link two Ag(I) ions. For framework isomers **54** and **55**, each $M_2L_2$ ring is directly connected with two adjacent ones *via* two *cis*-arms coordinating to Ag(I) ions from two neighbouring rings, leading to the formation of new 1D chains, in which the counter anions $ClO_4^-$ and $BF_4^-$ with a tetrahedral geometry do not participate in the formation of 1D chains. Compared with **54** and **55**, for **56**, the $M_2L_2$ rings are combined *via* the bonding of other Ag(I) ions and two *cis*-arms from two neighbouring rings, resulting in the

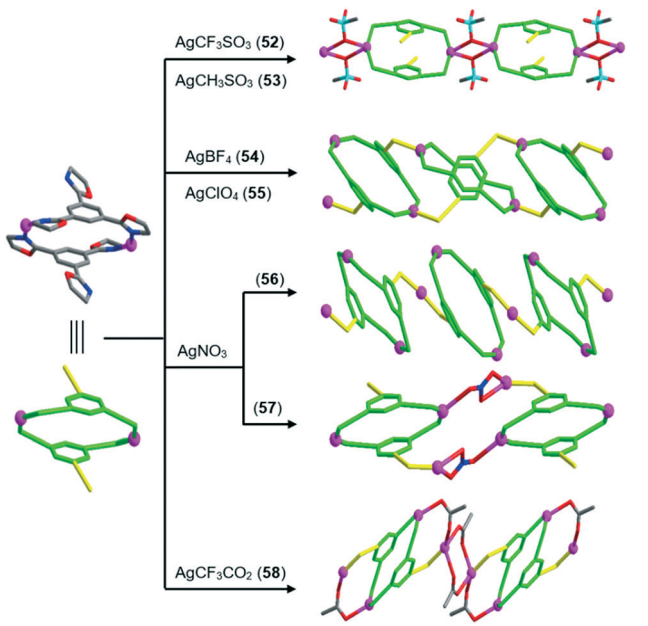


Fig. 9 1D chain structures of CPs **52**–**58** with $Ag_2(L2)_2$ subunits. Adapted from ref. 18*a* and 36.

formation of a new 1D chain, in which nitrate anions serve as terminal ligands. In contrast to the terminal nitrate anions in **56**, each nitrate anion in **57** acts as a bridging ligand, which is bound to two Ag(I) ions: one is from the $M_2L_2$ metallocycle and the other is bonded to a *cis*-arm from the adjacent $M_2L_2$ metallocycle. For **58**, each *cis*-arm of the $M_2L_2$ metallocycle is first bonded to a Ag(I) ion, which is further solidified into the $M_2L_2$ ring *via* a bis-monodentate bridging $CF_3COO^-$ anion to form a new $[Ag_4(L2)_2(CF_3COO)_2]^{2+}$ SBU. Such SBUs are further linked together *via* two bis-monodentate bridging $CF_3COO^-$ anions to produce a new 1D chain. The results illustrate that different coordination abilities of anions play a critical role in the construction of CPs. On the other hand, in contrast to insoluble AgX (X = Cl, Br), CuX (X = Cl, Br) is soluble in acetonitrile. Thus the influence of anions, especially $Cl^-$ and $Br^-$ anions, on the final structures of Cu(I) CPs with the oxazoline-based L2 ligand was investigated, and the corresponding four Cu(I) CPs $[Cu_2(L2)_2(H_2O)](ClO_4)_2$ (**59**), $[Cu_2(L2)_2Cl]ClO_4\cdot(9/4)H_2O\cdot(3/4)CH_3CN$, (**60**), $[Cu_2(L2)Br_2]$ (**61**) and $[Cu_4(L2)_2Br_4]\cdot 2CH_3CN$ (**62**) were described (Fig. 10).[18b] Like the Ag(I) CPs **52**–**58**, the PBU of Cu(I) complexes with the exception of **60** is also an $M_2L_2$ metallocycle. **59** displays a 1D chain structure like that of **54** and **55**. **61** consists of $[Cu_4(L2)_2(Br)_4]$ SBUs, which are directly connected to 1D chains through $\mu_3$-$Br^-$ anions. **62** possesses a 1D chain structure analogous to that of Ag(I) **56**, whereas, different from the 1D chain structure of **56**, the 1D chains in **61** are further joined together by bridging $Br^-$ ions to generate a 3D structure. Interestingly, there are no $M_2L_2$ 16-membered metallocycles in **60**. In contrast, **60** features $M_4L_4$ cage-like subunits, which are further extended into a 2D layer structure *via* bridging $Cl^-$ anions.

### 3.3. Homoleptic coordination polymers with multi-functional oxazoline-based ligands

Introduction of multi-functional oxazoline-containing ligands can make more diverse structures of CPs. In 2004, Reiser *et al.* reported a chiral, flexible, $C_2$-symmetric, pentadentate bis(oxazoline) ligand L27, which was employed to investigate the chirality transfer from ligands to metal centers, thereby creating two chiral 1D spiral chains $[Cd_2(L27)X_4]$ [X = Cl (**63**), Br (**64**)].[37] It is noteworthy that **63** and **64** have similar 1D chain structures, which consist of achiral Cd-(μ-X) inorganic backbone and twisted L27 ligands (Fig. 11). Apparently, the helicity from **63** and **64**, originating from the superposition of mononuclear helicate [Cd(L27)], differs from that of spring-like spiral chains arising from angular ditopic oxazoline-based ligands and 2-connected Ag(I) ions as exhibited in **41**.

Like ligand L27, the aforementioned L8 is also a flexible multi-functional oxazoline-containing ligand. Aside from two discrete coordination complexes **12** and **13**, we have also reported four CPs with molecular formulas $[Ag(L8)]CF_3SO_3$ (**65** and **66**), $[Ag(L8)]NO_3\cdot 0.5CH_3OH$ (**67**) and $[Ag(L8)]BF_4$ (**68**), synthesized by reaction of the L8 ligand and the corresponding Ag(I) salts (Fig. 12).[23] Complexes **65** and **66** are supramolecular isomers. **65** features a 2D wave-like layer composed of 3-connected oxazoline-based L8 ligands and tetrahedral Ag(I) nodes. By replacing the methanol solution of **65** with a mixture of dichloromethane and acetonitrile, **66** was obtained, displaying a 1D double-stranded helix. In **66**, each L8 ligand adopting a twisted conformation first connects with two Ag(I) ions *via* two terminal N atoms to generate a 1D spring-like helical chain. Subsequently, free ethylenediamine groups chelate with Ag(I) ions from another 1D chain to generate an entwined double-stranded helix structure. Evidently, reaction solvents play a key role in the formation of CPs. Due to the lack of chiral induction and the absence of conglomeration, **65** crystallizes in a *meso* form. Although **67** and **68** have

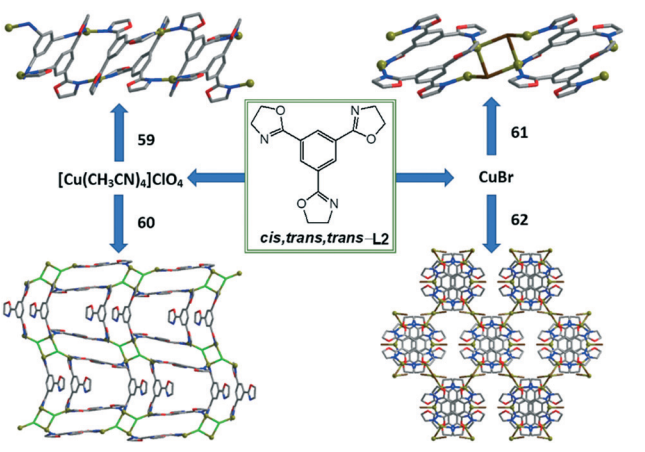


**Fig. 10** Crystal structures of CPs **59**–**62** with the *cis,trans,trans*-L2 ligand. Adapted from ref. 18*b*.

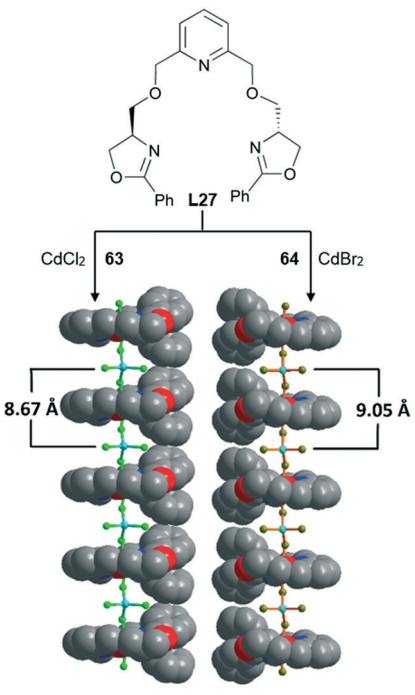


**Fig. 11** 1D chain structures of **63** and **64**, consisting of 1D inorganic chains and twisted L27 ligands. Adapted from ref. 37.

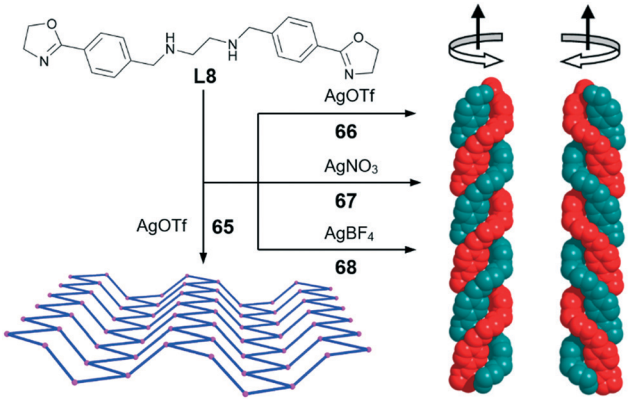


Fig. 12 2D layer of **65** with a (6,3) topology and 1D entwined double-stranded spiral chain structures of **66**–**68** with ligand L8. Adapted from ref. 23.

different counter anions from **66**, they have identical double-stranded helical structures. In other words, CPs **66**–**68** are also framework isomers. Surprisingly, the reaction of L8 with $HgI_2$ in the presence of tetrahydrofuran (THF) leads to the formation of a new Hg(II) CP $[HgI_2(L28)_2][Hg_2I_6]\cdot 2H_2O$ (**69**) with *in situ* generated 1,3-bis(4-(oxazolin-2-yl)benzyl)-2-(3-hydroxy-propyl)-imidazolinium (L28) salt (Fig. 13).[38] Detailed mechanism studies reveal that $CO_2$ first promotes the ring opening of THF, which accelerates the formation of intermediate imidazolidine. Finally, the intermediate imidazolidine was oxidatively dehydrogenated by $HgI_2$ to produce ligand L28, which further reacted with excess $HgI_2$ to yield the 1D chain structure of **69** as shown in Fig. 13.

In addition to the flexible multi-functional oxazoline-based ligands, we also designed a simple rigid ditopic oxazoline-based ligand 4-(oxazolin-2-yl)-pyridine (L29) (Fig. 14) which, according to the coordination vector principle, may be considered as an angular organic linker. Starting from L29 and $AgBF_4$, CP $[Ag(L29)](BF_4)$ (**70**) with a 1D zigzag chain structure was created, in which the 2-connected Ag(I) nodes take a nearly linear geometry.[39] Instead of $AgBF_4$ with $AgNO_3$, $AgSbF_6$ and $AgCF_3CO_2$ to react with L29, three distinct 2D CPs with formulas $[Ag_6(L29)_4(NO_3)_6]$ (**71**),

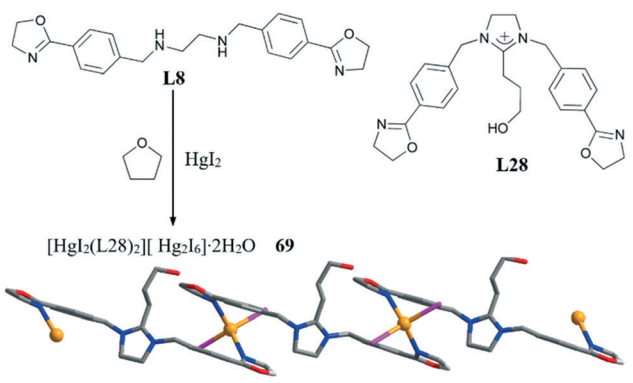


Fig. 13 1D chain structure of **69** with *in situ* generated ligand L28. Adapted from ref. 38.

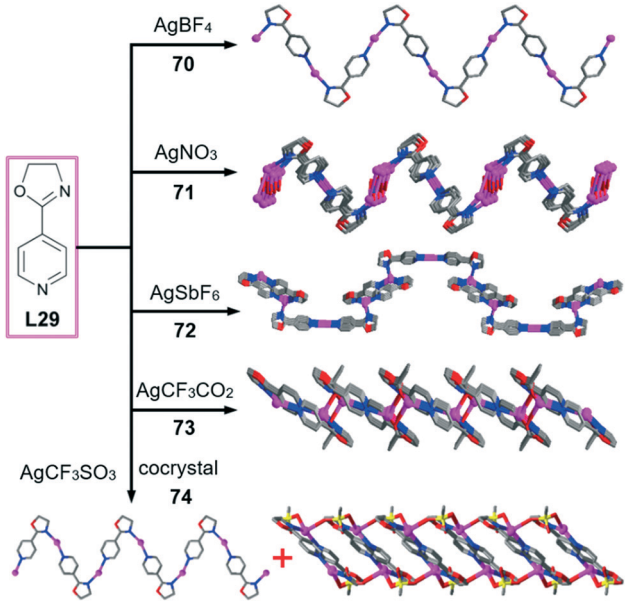


Fig. 14 Crystal structures of CPs **70**–**74** with ligand L29. Adapted from ref. 39.

$[Ag_3(L29)_4(CH_3CN)_2](SbF_6)_3(H_2O)$ (**72**) and $[Ag(L29)(OOCCF_3)]$ (**73**) were obtained. It is noticeable that both **71** and **72** possess a linear metallo-ligand [L29–Ag–L29], consisting of one 2-connected Ag(I) and two head-to-head coordinated L29 ligands. For **71**, the combination of Ag(I) ions with bis-monodentate bridging nitrate anions first yields a 1D inorganic chain $[Ag(NO_3)Ag]_n$, which further extends into a 2D wavy network by the linkage of *cis*,*trans*-conformational metallo-ligands. In contrast to **71**, the trapezoid 2D layer of **72** is made up of 1D zigzag chains similar to that of **70** and *cis*,*cis*-conformational bridging metallo-ligands, whereas the 2D sheet of **73** is composed of 1D zigzag chains like that of **70** and bridging trifluoromethyl acetate. Replacing $CH_3CO_2^-$ with $CH_3SO_3^-$ to react with L29, a cocrystal complex $[Ag(L29)(\mu_1\text{-}CH_3SO_3)][Ag(L29)(\mu_2\text{-}CH_3SO_3)]$ was yielded, which is made up of 1D zigzag chains like that of **70** and a 2D network analogous to that of **73**. Obviously, in the case of **70** and **72**, the anions $BF_4^-$ and $SbF_6^-$ serve only as free counter ions, while $NO_3^-$, $SO_3CF_3^-$ and $SO_3CH_3^-$ anions in **71**, **73** and **74** are involved in the coordination, which are responsible for the varied structures. All in all, combined with the above discussed examples, it can be preliminarily concluded that the coordination ability of anions plays a remarkable role compared to their size and shape in the construction of CSs and the coordination ability sequence is $X^-$ ($Cl^-$ and $Br^-$) > $CF_3COO^-$ > $CF(H)_3SO_3^-$ > $NO_3^-$ > $ClO_4^-$ ≈ $BF_4^-$ > $PF_6^-$ ≈ $SbF_6^-$.

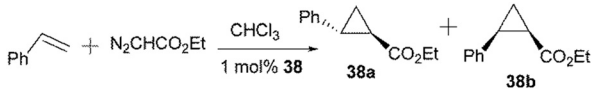


Scheme 14 Reaction of styrene and ethyl diazoacetate catalyzed by chiral Cu(I) helical chain **38**. Adapted from ref. 30*a*.

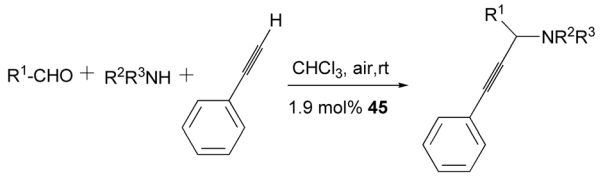


**Scheme 15** Three-component coupling reaction of aldehyde, alkyne and amine catalyzed by 1D zigzag chain **45**. Adapted from ref. 34*a*.

# 4. Properties of oxazoline-based coordination supramolecules

### 4.1. Luminescence properties of oxazoline-based discrete coordination complexes

It is known that luminescent Eu-based CSs have potential applications in the fields of chemical and biological sensing. For example, CSs **27** and **28** are Eu-based tetrahedral cages with inherent cavities (Fig. 4), which can accommodate small guest molecules/ions and thus facilitate their luminescence recognition.[26] **27** is an $M_4L_6$ cage with excellent photoluminescence properties, which displays highly efficient and selective detection toward explosive picric acid at the ppb level *via* fluorescence quenching. Compared with **27**, **28** is an $M_4L_4$ cage with $C_3$-symmetric L15 exhibiting excellent intraligand charge transfer (ILCT) sensitization. Based on the ILCT transition of the L15 ligand, **28** displays unusually dual-responsive detection toward $I^-$ based on a turn-off effect and $Cu^{2+}$ based on a turn-on effect. In contrast to achiral **27** and **28**, Eu-oxazoline-based CSs **30**–**33** are all chiral, which exhibit large circularly polarized luminescence (CPL), among which triangles **30** and **31** have the highest intensity.[27c,d]

### 4.2. Catalytic properties of oxazoline-based coordination polymers

As mentioned in the Introduction, oxazoline ligands have been widely employed in catalytic fields in the past years. Hence, incorporation of oxazoline-based ligands into CPs for catalysis can readily realize the heterogenization of homogeneous catalysts. However, there are two disadvantages that limit their further application. First, the metal centers of oxazoline-based CP catalysts are mainly soft Lewis acids: Cu(I), Ag(I) and Hg(II). Second, there are no reported 3D porous oxazoline-based CPs. That is, except for **51**, for other CP catalysts, there is no synergistic effect between the pore size and catalytic site. The following is the reported catalytic application of oxazoline-based CPs.

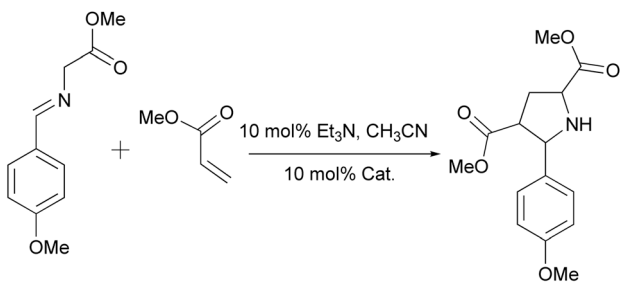


**Scheme 16** Cycloaddition reaction of methyl 2-(4-methoxybenzylideneamino)acetate and methyl acrylate catalyzed by the Ag(I) CPs **49**, **50** and **51** in $CH_3CN$. Adapted from ref. 35.

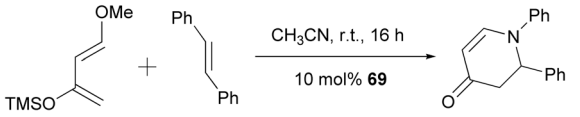


**Scheme 17** Aza-Diels–Alder reaction of *N*-benzylideneaniline and Danishefsky's diene catalyzed by Hg(II) CP **69**. Adapted from ref. 38.

Chiral CP [Cu(L20$^{SS}$)]OTf (**38**) discussed in section 3.1 (Scheme 12) can effectively catalyse enantioselective cyclopropanation of olefins by ethyl diazoacetate. For example, when styrene was subjected to this reaction with ethyl diazoacetate in the presence of **38** (1 mol%), enantioselective ethyl cyclopropanecarboxylates **38a** and **38b** were obtained in a 73 : 27 ratio both with a 98% *ee* value (Scheme 14).[30a]

Ag(I) oxazoline-based CP **45** (Fig. 7) has been applied in the three-component coupling reaction of aldehyde, alkyne and amine in air rather than in a $N_2$ atmosphere using other catalysts (Scheme 15). Under the optimal conditions, the range of this three-component coupling reaction by using different amines and aldehydes to react with phenylacetylene was examined. The results reveal that the cyclic and acyclic secondary aliphatic amines and aliphatic aldehydes have high reactivity. More importantly, the catalyst **45** can be conveniently recycled by simple filtration and reused at least four times with no obvious decrease in its catalytic activity.[34a]

In addition, **49**, **50** and **51** (Fig. 8) were further used to catalyse the cycloaddition reactions between imino esters and methyl acrylate (Scheme 16). Among the three CPs, channel-structured **51** gives the highest activity, which is ascribed to the synergistic effect of the pores and catalytic sites. Furthermore, during the catalytic reaction, the structures of the three complexes show good solvent stability, which are ascertained by PXRD.[35] In 2017, we found that *in situ* generated Hg(II) CP **69** (Fig. 13) is an active catalyst for the aza-Diels–Alder reaction between *N*-benzylideneaniline and Danishefsky's diene (Scheme 17). When 10 mol% **69** was used, 99% conversion was observed.[38]

# 5. Conclusions

Coordination supramolecules (CSs) are still a flourishing research field due to their fascinating structures, interesting properties and potential applications in many aspects. However, the insight into the relationship between their structures and properties remains unclear for researchers. This highlight presented the progress of oxazoline-based CSs, including discrete coordination complexes and coordination polymers (CPs), together with their applications in luminescence and catalysis.

For discrete CSs such as cages, rectangles and helicates, oxazoline-containing ligands with $C_2$ and $C_3$ symmetry are useful. They can be directionally synthesized by a molecular

clip approach based on ligand-directed symmetry interactions. Particularly, tetrahedral cages with large cavities, which can accommodate guest molecules and ions, can be obtained by assembly of $C_2/C_3$-symmetric multi-topic ligands with oxazoline-containing chelating moieties and naked $Ln^{3+}$ ions, which can be used as sensors for detecting ions. It is noteworthy that the presence of bulky 4-substituted groups of the oxazoline ring can facilitate the formation of discrete coordination complexes.

On the other hand, reported oxazoline-based CPs mainly possess 1D chain structures and a few 2D networks. The reason can be ascribed to the *ortho*-positioned N-donor atom in the oxazoline moiety, which hinders the outward expansion of the structures. In contrast, an analogous tib ligand can form porous 3D frameworks.[40] Furthermore, although some of the oxazoline-based CPs have been utilized as heterogeneous catalysts, reports on the catalytic reaction type and their efficiency are still scarce. In conclusion, the study on oxazoline-based CSs is still in its infancy and there are ample opportunities for further exploration.

## Conflicts of interest

There are no conflicts to declare.

## Acknowledgements

This work was financially supported by the National Natural Science Foundation of China (grant no. 21331002 and 21201111) and the National Basic Research Program of China (grant no. 2017YFA0303504). This work was also supported by a project funded by the Priority Academic Program Development of Jiangsu Higher Education Institutions.

## Notes and references

1 (*a*) R. W. Saalfrank, H. Maid and A. Scheurer, *Angew. Chem., Int. Ed.*, 2008, **47**, 8794–8824; (*b*) T. R. Cook and P. J. Stang, *Chem. Rev.*, 2015, **115**, 7001–7045; (*c*) W. Wang, Y.-X. Wang and H.-B. Yang, *Chem. Soc. Rev.*, 2016, **45**, 2656–2693; (*d*) M. Li, D. Li, M. O'Keeffe and O. M. Yaghi, *Chem. Rev.*, 2014, **114**, 1343–1370; (*e*) T. Kitao, Y. Zhang, S. Kitagawa, B. Wang and T. Uemura, *Chem. Soc. Rev.*, 2017, **46**, 3108–3133; (*f*) R. Haldar and T. K. Maji, *CrystEngComm*, 2013, **15**, 9276–9295; (*g*) Y. He, B. Lin, M. O'Keeffe and B. Chen, *Chem. Soc. Rev.*, 2014, **43**, 5618–5656.

2 (*a*) J. A. Mason, M. Veenstra and J. R. Long, *Chem. Sci.*, 2014, **5**, 32–51; (*b*) S. Chaemchuen, N. A. Kabir, K. Zhou and F. Verpoort, *Chem. Soc. Rev.*, 2013, **42**, 9304–9332; (*c*) Y. He, W. Zhou, G. Qian and B. Chen, *Chem. Soc. Rev.*, 2014, **43**, 5657–5678; (*d*) T. A. Makal, J.-R. Li, W. Lu and H.-C. Zhou, *Chem. Soc. Rev.*, 2012, **41**, 7761–7779; (*e*) M. Gallo and D. Glossman-Mitnik, *J. Phys. Chem. C*, 2009, **113**, 6634–6642.

3 (*a*) D. Bradshaw, A. Garai and J. Huo, *Chem. Soc. Rev.*, 2012, **41**, 2344–2381; (*b*) B. Li, H. Wang and B. Chen, *Chem. – Asian J.*, 2014, **9**, 1474–1498; (*c*) B. R. Pimentel, A. Parulkar, E.-K. Zhou, N. A. Brunelli and R. P. Lively, *ChemSusChem*, 2014, **7**, 3202–3240; (*d*) Z. Bao, G. Chang, H. Xing, R. Krishna, Q. Ren and B. Chen, *Energy Environ. Sci.*, 2016, **9**, 3612–3641.

4 (*a*) K. Müller-Buschbaum, F. Beuerle and C. Feldmann, *Microporous Mesoporous Mater.*, 2015, **216**, 171–199; (*b*) Z. Hu, B. J. Deibert and J. Li, *Chem. Soc. Rev.*, 2014, **43**, 5815–5840; (*c*) W. P. Lustig, S. Mukherjee, N. D. Rudd, A. V. Desai, J. Li and S. K. Ghosh, *Chem. Soc. Rev.*, 2017, **46**, 3242–3285; (*d*) L. V. Meyer, F. Schönfeld and K. Müller-Buschbaum, *Chem. Commun.*, 2014, **50**, 8093–8108; (*e*) L. E. Kreno, K. Leong, O. K. Farha, M. Allendorf, R. P. V. Duyne and J. T. Hupp, *Chem. Rev.*, 2012, **112**, 1105–1125; (*f*) I. Stassen, N. Burtch, A. Talin, P. Falcaro, M. Allendorf and R. Ameloot, *Chem. Soc. Rev.*, 2017, **46**, 3185–3241.

5 (*a*) J. Liu, L. Chen, H. Cui, J. Zhang, L. Zhang and C.-Y. Su, *Chem. Soc. Rev.*, 2014, **43**, 6011–6061; (*b*) A. H. Chughtai, N. Ahamd, H. A. Younus, A. Laypkov and F. Verpoort, *Chem. Soc. Rev.*, 2015, **44**, 6804–6849; (*c*) Y.-B. Huang, J. Liang, X.-S. Wang and R. Cao, *Chem. Soc. Rev.*, 2017, **46**, 126–157; (*d*) S. Ou and C.-D. Wu, *Inorg. Chem. Front.*, 2014, **1**, 721–734; (*e*) J. Jiang and O. M. Yaghi, *Chem. Rev.*, 2015, **115**, 6966–6997; (*f*) W. Wang, Y.-X. Wang and H.-B. Yang, *Chem. Soc. Rev.*, 2016, **45**, 2656–2693; (*g*) S. H. A. M. Leenders, R. Gramage-Doria, B. D. Bruin and J. N. H. Reek, *Chem. Soc. Rev.*, 2015, **44**, 433–448.

6 (*a*) T. Hang, W. Zhang, H.-Y. Ye and R.-G. Xiong, *Chem. Soc. Rev.*, 2011, **40**, 3577–3598; (*b*) W. Zhang and R.-G. Xiong, *Chem. Rev.*, 2012, **112**, 1163–1195; (*c*) L. R. Mingabudinova, V. V. Vinogradov, V. A. Milichko, E. Hey-Hawkins and A. V. Vinogradov, *Chem. Soc. Rev.*, 2016, **45**, 5408–5431; (*d*) C. Wang, T. Zhang and W. Lin, *Chem. Rev.*, 2012, **112**, 1084–1104; (*e*) H. Xu, R. Chen, Q. Sun, W. Lai, Q. Su, W. Huang and X. Liu, *Chem. Soc. Rev.*, 2014, **43**, 3259–3302.

7 (*a*) N. Ahmad, H. A. Younus, A. H. Chughtai and F. Verpoort, *Chem. Soc. Rev.*, 2015, **44**, 9–25; (*b*) J. Zhou, G. Yu and F. Huang, *Chem. Soc. Rev.*, 2017, **46**, 7021–7053; (*c*) W. Chen and C. Wu, *Dalton Trans.*, 2018, **47**, 2114–2133; (*d*) J. D. Rocca, D. Liu and W. Lin, *Acc. Chem. Res.*, 2011, **44**, 957–968.

8 (*a*) L. Brammer, *Chem. Soc. Rev.*, 2004, **33**, 476–489; (*b*) M. W. Hosseini, *Acc. Chem. Res.*, 2005, **38**, 313–323; (*c*) D. J. Tranchemontagne, J. L. Mendoza-Cortés, M. O'Keeffe and O. M. Yaghi, *Chem. Soc. Rev.*, 2009, **38**, 1257–1283.

9 (*a*) R. G. Pearson, *J. Am. Chem. Soc.*, 1963, **85**, 3533–3539; (*b*) T. Devic and C. Serre, *Chem. Soc. Rev.*, 2014, **43**, 6097–6115.

10 (*a*) Z. Zhang, Z.-Z. Yao, S. Xiang and B. Chen, *Energy Environ. Sci.*, 2014, **7**, 2868–2899; (*b*) J. Liu, P. K. Thallapally, B. P. McGrail, D. R. Brown and J. Liu, *Chem. Soc. Rev.*, 2012, **41**, 2308–2322; (*c*) C. S. Diercks, Y. Liu, K. E. Cordova and O. M. Yaghi, *Nat. Mater.*, 2018, **17**, 301–307; (*d*) R. W. Flaig, T. M. Osborn Popp, A. M. Fracaroli, E. A. Kapustin, M. J. Kalmutzki, R. M. Altamimi, F. Fathieh, J. A. Reimer and O. M. Yaghi, *J. Am. Chem. Soc.*, 2017, **139**, 12125–12128.

11 (*a*) J. A. Thompson, C. R. Blad, N. A. Brunelli, M. E. Lydon, R. P. Lively, C. W. Jones and S. Nair, *Chem. Mater.*, 2012, **24**, 1930–1936; (*b*) X.-Z. Li, X.-P. Zhou, D. Li and Y.-G. Yin, *CrystEngComm*, 2011, **13**, 6759–6765.

 

12 (*a*) G. Yang and W. Zhang, *Chem. Soc. Rev.*, 2018, **47**, 1783–1810; (*b*) G. C. Hargaden and P. J. Guiry, *Chem. Rev.*, 2009, **109**, 2505–2550; (*c*) R. Rasappan, D. Laventine and O. Reiser, *Coord. Chem. Rev.*, 2008, **252**, 702–714.

13 (*a*) S. D. Bennett, B. A. Core, M. P. Blake, S. J. A. Pope, S. J. A. Pope, P. Mountford and B. D. Ward, *Dalton Trans.*, 2014, **43**, 5871–5885; (*b*) M. Gómez, G. Muller and M. Rocamora, *Coord. Chem. Rev.*, 1999, **193-195**, 769–835; (*c*) P. Braunstein and F. Naud, *Angew. Chem., Int. Ed.*, 2001, **40**, 680–699.

14 B. D. Ward and L. H. Gade, *Chem. Commun.*, 2012, **48**, 10587–10599.

15 (*a*) S. Leininger, B. Olenyuk and P. J. Stang, *Chem. Rev.*, 2000, **100**, 853–908; (*b*) D. L. Caulder and K. N. Raymond, *J. Chem. Soc., Dalton Trans.*, 1999, 1185–1200; (*c*) D. L. Caulder and K. N. Raymond, *Acc. Chem. Res.*, 1999, **32**, 975–982; (*d*) P. J. Stang and B. Olenyuk, *Acc. Chem. Res.*, 1997, **30**, 502–518; (*e*) M. Fujita, K. Umemoto, M. Yoshizawa, M. Fujita, T. Kusukawa and K. Biradha, *Chem. Commun.*, 2001, 509–518; (*f*) C.-Y. Su, Y.-P. Cai, C.-L. Chen, M. D. Smith, W. Kaim and H.-C. Loye, *J. Am. Chem. Soc.*, 2003, **125**, 8595–8613.

16 (*a*) M. Fujita, S. Nagao and K. Ogura, *J. Am. Chem. Soc.*, 1995, **117**, 1649–1650; (*b*) W.-Y. Sun, J. Fan, T.-a. Okamura, K.-B. Yu and N. Ueyama, *Chem. – Eur. J.*, 2001, **7**, 2557–2562.

17 H.-J. Kim, D. Moon, M. S. Lah and J.-I. Hong, *Angew. Chem., Int. Ed.*, 2002, **41**, 3174–3177.

18 (*a*) Y.-Q. Huang, Z.-L. Shen, T.-A. Okamura, Y. Wang, X.-F. Xiao, W.-Y. Sun, J.-Q. Yu and N. Ueyama, *Dalton Trans.*, 2008, 204–213; (*b*) Y.-Q. Huang, Z.-L. Shen, X.-Y. Zhou, T.-A. Okamura, Z. Su, J. Fan, W.-Y. Sun, J.-Q. Yu and N. Ueyama, *CrystEngComm*, 2010, **12**, 4328–4338.

19 J. Fan, W.-Y. Sun, T.-A. Okamura, W.-X. Tang and N. Ueyama, *Inorg. Chem.*, 2003, **42**, 3168–3175.

20 J. Fan, H.-F. Zhu, T.-A. Okamura, W.-Y. Sun, W.-X. Tang and N. Ueyama, *Chem. – Eur. J.*, 2003, **9**, 4724–4731.

21 S. Hiraoka, T. Tanaka and M. Shionoya, *J. Am. Chem. Soc.*, 2006, **128**, 13038–13039.

22 S. Hiraoka, M. Goda and M. Shionoya, *J. Am. Chem. Soc.*, 2009, **131**, 4592–4593.

23 Y.-Q. Huang, G.-X. Liu, X.-Y. Zhou, T.-A. Okamura, Z. Su, J. Fan, W.-Y. Sun, J.-Q. Yu and N. Ueyama, *New J. Chem.*, 2010, **34**, 2436–2444.

24 Y. Zhao, L.-L. Li, G.-C. Lv, X. Zhou and W.-Y. Sun, *Inorg. Chim. Acta*, 2012, **392**, 38–45.

25 (*a*) C. Provent, S. Hewage, G. Brand, G. Bernardinelli, L. J. Charbonnière and A. F. Williams, *Angew. Chem., Int. Ed. Engl.*, 1997, **36**, 1287–1289; (*b*) G. M. Borrajo-Calleja, E. d. Julián, E. Bayón, J. Díez, E. Lastra, I. Merino and M. P. Gamasa, *Inorg. Chem.*, 2016, **55**, 8794–8807.

26 (*a*) C.-L. Liu, L.-P. Zhou, D. Tripathy and Q.-F. Sun, *Chem. Commum.*, 2017, **53**, 2459–2462; (*b*) C.-L. Liu, R.-L. Zhang, C.-S. Lin, L.-P. Zhou, L.-X. Cai, J.-T. Kong, S.-Q. Yang, K.-L. Han and Q.-F. Sun, *J. Am. Chem. Soc.*, 2017, **139**, 12474–12479.

27 (*a*) Y. Bretonnière, M. Mazzanti, J. Pécaut and M. M. Olmstead, *J. Am. Chem. Soc.*, 2002, **124**, 9012–9013; (*b*) X. Y. Chen, Y. Bretonnière, J. Pecaut, D. Imbert, J. C. Bunzli and M. Mazzanti, *Inorg. Chem.*, 2007, **46**, 625–637; (*c*) G. Bozoklu, C. Gateau, D. Imbert, J. Pécaut, K. Robeyns, Y. Filinchuk, F. Memon, G. Muller and M. Mazzanti, *J. Am. Chem. Soc.*, 2012, **134**, 8372–8375; (*d*) G. Bozoklu, C. Marchal, C. Gateau, J. Pécaut, D. Imbert and M. Mazzanti, *Chem. – Eur. J.*, 2010, **16**, 6159–6163.

28 H. Y. Lee, J. Park, M. S. Lah and J.-I. Hong, *Chem. Commun.*, 2007, 5013–5015.

29 (*a*) S. Hiraoka, K. Hirata and M. Shionoya, *Angew. Chem., Int. Ed.*, 2004, **43**, 3814–3818; (*b*) S. Hiraoka, E. Okuno, T. Tanaka, M. Shiro and M. Shionoya, *J. Am. Chem. Soc.*, 2008, **130**, 9089–9098.

30 (*a*) D. A. Evans, K. A. Woerpel and M. J. Scott, *Angew. Chem., Int. Ed. Engl.*, 1992, **31**, 430–432; (*b*) S. Ma and S. Wu, *Chin. J. Chem.*, 2000, **18**, 444–446; (*c*) S. Ma and S. Wu, *New J. Chem.*, 2001, **25**, 1337–1341.

31 Y. Zhao, L. Luo, C. Liu, M. Chen and W.-Y. Sun, *Inorg. Chem. Commun.*, 2011, **14**, 1145–1148.

32 E. Vega, E. D. Julián, G. Borrajo, J. Díez, E. Lastra and M. P. Gamasa, *Polyhedron*, 2015, **94**, 59–66.

33 H.-W. Kuai, X.-C. Cheng, D.-H. Li, T. Hu and X.-H. Zhu, *J. Solid State Chem.*, 2015, **228**, 65–75.

34 (*a*) Y. Zhao, X. Zhou, T.-A. Okamura, M. Chen, Y. Lu, W.-Y. Sun and J.-Q. Yu, *Dalton Trans.*, 2012, **41**, 5889–5896; (*b*) C. Liu, Y. Zhao, L.-L. Zhai, G.-C. Lv and W.-Y. Sun, *J. Coord. Chem.*, 2012, **65**, 165–175.

35 Y. Zhao, K. Chen, J. Fan, T.-A. Okamura, Y. Lu, L. Luo and W.-Y. Sun, *Dalton Trans.*, 2014, **43**, 2252–2258.

36 Y.-Q. Huang, X.-Y. Zhou, Z.-L. Shen, G.-X. Liu, J.-Q. Yu and W.-Y. Sun, *Acta Chim. Sin.*, 2007, **65**, 1381–1384.

37 M. Seitz, A. Kaiser, S. Stempfhuber, M. Zabel and O. Reiser, *J. Am. Chem. Soc.*, 2004, **126**, 11426–11427.

38 Y.-Q. Huang, Y. Zhao, P. Wang, T.-A. Okamura, B. N. Laforteza, Y. Lu, W.-Y. Sun and J.-Q. Yu, *Dalton Trans.*, 2017, **46**, 12430–12433.

39 Y. Zhao, L.-L. Zhai, J. Fan, K. Chen and W.-Y. Sun, *Polyhedron*, 2012, **46**, 16–24.

40 (*a*) Y.-X. Sun and W.-Y. Sun, *CrystEngComm*, 2015, **17**, 4045–4063; (*b*) X.-L. Zhao and W.-Y. Sun, *CrystEngComm*, 2014, **16**, 3247–3258.